

Stability and thermodynamics of brane black holes

E. Abdalla, B. Cuadros-Melgar,^y and A. B. Pavan^z
Instituto de Física, Universidade de São Paulo
C.P. 66318, 05315-970, São Paulo-SP, Brazil

C. Molina^x
Escola de Artes, Ciências e Humanidades, Universidade de São Paulo
Av. Arlindo Bettio 1000, CEP 03828-000, São Paulo-SP, Brazil

We consider scalar and axial gravitational perturbations of black hole solutions in brane world scenarios. We show that perturbation dynamics is surprisingly similar to the Schwarzschild case with strong indications that the models are stable. Quasinormal modes and late-time tails are discussed. We also study the thermodynamics of these scenarios verifying the universality of Bekenstein's entropy bound as well as the applicability of 't Hooft's brickwall method.

PACS numbers: 04.70.Dy, 98.80.Cq, 97.60.Lf, 04.50.+h

I. INTRODUCTION

The extra dimensions idea had its origin in the seminal works by Kaluza and Klein in the 20's [1] and gained momentum in the context of string theory in the last decades [2]. Recent developments on higher-dimensional gravity resulted in a number of interesting theoretical ideas such as the brane world concept. The essence of this string inspired model is that Standard Model fields are confined to a three dimensional hypersurface, the brane, while gravity propagates in the full spacetime, the bulk. The simplest models in this context (abbreviated here as RS I and RS II), proposed by Randall and Sundrum [3], describe our world as a domain wall embedded in a Z_2 -symmetric five dimensional anti-de Sitter (AdS) spacetime. The RS I model proposes a mechanism to solve the hierarchy problem by a small extra dimension, while the RS II model considers an infinite extra dimension with a warp factor which ensures the localization of gravity on our brane.

Black holes are important sources of gravitational waves that are expected to be detected by the current and upcoming generation of experiments. This will open up a new window for testing modifications of general relativity. The simplest case of gravitational collapse in the standard four dimensional world is described by the 4-dimensional Schwarzschild metric. In the 5-dimensional scenario it would be natural to ask whether matter confined on the brane after undergoing gravitational collapse can still be described by a Schwarzschild-type metric. The most natural generalization in the RS II model corresponds to a black string in five in the fifth dimension, whose induced metric on the brane is purely Schwarzschild [4]. However, although the cur-

vature scalars are everywhere finite, the Kretschmann scalar diverges at the AdS horizon at infinity, which turns the above solution into a physically unsuitable object.

It has been argued that there exists a localized black cigar solution with a finite extension along the extra dimension due to a Gregory-Laflamme [5] type of instability near the AdS horizon. A class of such a solution has been found by Casadio et al. [6, 7] using the projected Einstein equations on the brane derived by Shiromizu et al. [8]. It has the desired "pancake" horizon structure ensuring a non-singular behavior in the curvature and Kretschmann scalars at least until the order of the multipole expansion considered there. In fact, this solution belongs to a class of black hole solutions found later by Bronnikov et al. [9], who also classified several possible brane black holes obtained from the Shiromizu et al. projected equations [8] in two families according to the horizon order. For such spacetimes only horizons of order 1 or 2 are possible, but not higher than that.

In this paper we are interested in the study of black holes from the point of view of a brane observer, as ourselves. We analyze some characteristics of Bronnikov et al. solutions. Firstly, some aspects of the thermodynamics are studied. Black Hole Thermodynamics was constructed when Bekenstein proposed the proportionality law between the entropy and the horizon area [10]. The discovery of Hawking radiation validated this proposal and established the proportionality factor $1/4$ in a precise way [11] leading to the well-known Bekenstein-Hawking formula,

$$S_{BH} = \frac{A_{rea}}{4G} : \quad (1)$$

One way to compute the entropy based on a semi-classical description of a scalar field was proposed by 't Hooft [12] and it is known as the brick wall method, which was frequently used later in several contexts [13]. When applying this method to a Schwarzschild black hole, 't Hooft found that the entropy was proportional to the area, as expected, but additionally it had a l^2 correction, being the proper distance from the horizon to

arXiv:gr-qc/0604033v2 27 Aug 2006

^Electronic address: eabdalla@fma.ifusp.br

^yElectronic address: berthaa@fma.ifusp.br

^zElectronic address: alan@fma.ifusp.br

^xElectronic address: cmolina@usp.br

the wall. This term was later interpreted as a one-loop correction to the Bekenstein-Hawking formula, since it can be absorbed as a renormalization of the gravitational coupling constant G [14].

Another interesting feature of black hole thermodynamics is the existence of an upper bound on the entropy of any neutral system of energy E and maximal radius R in the form $S \leq 2\pi ER$, proposed by Bekenstein [15]. This bound becomes necessary in order to enforce the generalized second law of thermodynamics (GSL).

Besides thermodynamical results, we also consider the response of a brane black hole perturbation which should represent some damped oscillating signal. It can be decomposed with Laplace transformation techniques into a set of so-called quasinormal modes (QNM). The QNMs of black holes are important because they dominate in the intermediate late-time decay of a perturbation and do not depend upon the way they were excited. They depend only on the parameters of a black hole and are, therefore, the "footprints" of this structure. The time-independent problem for perturbations of a brane black hole turns out to be quite similar to that for a black hole: one has to find the solutions of the wave-like equations satisfying the appropriate boundary conditions, which we shall further discuss in detail.

The paper is organized as follows, in Sec. II the brane black holes are presented. Sec. III discusses the thermodynamical properties of the solutions thus considered. Sec. IV treats the question of perturbation and stability of these objects. Wave-like equations for the perturbations are derived. In Sec. V an analysis of the quasinormal modes and late-time behavior is developed. In Sec. VI we summarize our results, and some final comments are made.

II. BRANE BLACK HOLE SOLUTIONS

The vacuum Einstein equations in 5 dimensions, when projected on a 4-dimensional spacetime and after introducing gaussian normal coordinates (x , with $\mu = 0 \dots 3$, and z), lead to the gravitational equation on the 3-brane given by [8]

$$R^{(4)} = \kappa_4 g^{(4)} E \quad (2)$$

where κ_4 is the brane cosmological constant, and E is proportional to the (traceless) projection on the brane of the 5-dimensional Weyl tensor.

The only combination of the Einstein equations in a brane world that can be written unambiguously without specifying E is their trace [6, 7, 9],

$$R^{(4)} = 4\Lambda_4 : \quad (3)$$

It is clear that this equation, also known as the hamiltonian constraint in the ADM decomposition of the metric, is a weaker restriction than the purely 4-dimensional

equation $R = 0$, which, in fact, is equivalent to Eq. (2), provided that we know the structure of E .

In order to obtain four dimensional solutions of Eq. (3), we choose the spherically symmetric form of the 4-dimensional metric given by

$$ds^2 = -A(r)dt^2 + \frac{dr^2}{B(r)} + r^2(d\theta^2 + \sin^2\theta d\phi^2) \quad (4)$$

We relax the condition $A(r) = B(r)$, which is accidentally verified in four dimensions but, in fact, there is no reason for it to continue to be valid in this scenario. In this spirit, black hole and worm hole solutions [6, 9, 16, 17] as well as star solutions on the brane [18] have been obtained in the last years. We should mention that even without relaxing this condition, previous solutions have also been found [19, 20].

In this context the hamiltonian constraint can be written explicitly in terms of A and B as [6, 9]

$$B \left(\frac{A''}{A} - \frac{1}{2} \frac{A'^2}{A^2} + \frac{1}{2} \frac{A^0 B^0}{A B} + \frac{2}{r} \frac{B^0}{B} + \frac{A^0}{A} \right) - \frac{2}{r^2} (1 - B) = 4\Lambda_4 ; \quad (5)$$

with prime ($'$) denoting differentiation with respect to r .

We will center our attention in the black hole type solutions which can be obtained by one of the following algorithms BH1 and BH2. These are subclasses of the corresponding algorithms in [9] (where the parameter s in this reference is set to 1).

First Algorithm (BH1): Specify a function $A(r)$, positive and analytical in a neighborhood of the event horizon $R[r]$, in such a way that $4A + rA^0 > 0$ in $R[r]$, and $A \rightarrow 0$ as $r \rightarrow r_h$. Then $B(r)$ is given by the general solution of (5) with vanishing brane cosmological constant,

$$B(r) = \frac{2Ae^3}{r(4A + rA^0)^2} \int_{r_h}^r (4A + rA^0)(2 - r^2 R) e^{-3} dr + C ; \quad (6)$$

where C is an integration constant and

$$R(r) = \frac{A^0}{4A + rA^0} dr : \quad (7)$$

For $C = 0$ we have a black hole metric with a horizon at $r = r_h$, which is simple if $C > 0$ and of the order $2 + p$ if both $C = 0$, and Q has the behavior,

$$Q(r) = 2 - r^2 R \rightarrow 0 \text{ as } r \rightarrow r_h ; p \geq 2, N : \quad (8)$$

Second Algorithm (BH2): Specify a function $A(r)$, positive and analytical in a neighborhood of the event horizon $R[r]$, in such a way that $4A + rA^0 > 0$ in $R[r]$, and $A \rightarrow 0$ as $r \rightarrow r_h$. Then $B(r)$ is again given by (6). The black hole metric appears when $C = 0$ with

a horizon at $r = r_h$ of the order $2 + p$ if $Q(r)$ behaves according to (8).

Both algorithms lead to double horizons in the case $C = 0$, if $Q(r_h) > 0$. A case in point of the first algorithm is the solution with the metric element $A(r)$ having the usual form of a Schwarzschild black hole found by Casadio, Fabbri, and Mazzacurati (CFM solution) [6, 7] given by

$$\begin{aligned} A(r) &= 1 - \frac{2M}{r}; \\ B(r) &= \frac{(1 - \frac{2M}{r})(1 - \frac{M}{2r})}{1 - \frac{3M}{2r}}; \end{aligned} \quad (9)$$

where \int is an integration constant. The event horizon is localized at $r_h = 2M$ and the singularity at $r = 3M/2$ instead of $r = 0$. Notice that the Schwarzschild solution is recovered with $\int = 3$. In this work we are restricted to the case when $\int < 4$.

Another interesting example of this algorithm is the metric with zero Schwarzschild mass [9] given by

$$\begin{aligned} A(r) &= 1 - \frac{h^2}{r^2}; \quad h > 0; \\ B(r) &= 1 - \frac{h^2}{r^2} - 1 + \frac{C}{2r^2} - \frac{h}{r^2}; \end{aligned} \quad (10)$$

whose horizon $r = h$ is simple if $C > 0$ and double if $C = 0$. The singularity occurs at $r = h/\sqrt{2}$. This example shows that in the brane world context a black hole may exist without matter and without mass, only as a tidale ect from the bulk gravity. However, there is a special situation when h^2 can be related to a 5-dimensional mass, namely, $C = h$. In this case Eq. (10) is the induced metric of a 5-dimensional Schwarzschild black hole, as described in [21], where the chosen background was ADD-type.

III. BLACK HOLE THERMODYNAMICS

In order to study the thermodynamical properties of the brane black holes generated by the BH1 and BH2 algorithms, we use the following expressions of the metric coefficients near the horizon

$$\begin{aligned} A(r) &= A_1(r - r_h) + O((r - r_h)^2) \\ B(r) &= B_1C(r - r_h) + B_2(r - r_h)^2 + O((r - r_h)^3); \end{aligned} \quad (11)$$

for BH1 algorithm with $A_1; B_1; B_2 > 0$ and C being an integration constant that defines the black hole family, and

$$\begin{aligned} A(r) &= A_2(r - r_h)^2 + O((r - r_h)^3); \\ B(r) &= B_3C + B_4(r - r_h)^2 + B_5(r - r_h)^3 \\ &\quad + O((r - r_h)^4); \end{aligned} \quad (12)$$

for BH2 algorithm, being C the family parameter again.

We will show here the calculation for the BH2 family, which turns out to be more interesting, since the metric coefficients expansion (12) is different from the standard one (11). However, we will display certain quantities for both families wherever it is relevant.

We first consider the issue of the entropy bound. The surface gravity at the event horizon is given by

$$\kappa = \begin{cases} \frac{1}{2} \frac{p}{A_1 B_1 C} & \text{for BH1 family;} \\ \frac{1}{2} \frac{p}{A_2 B_3 C} & \text{for BH2 family;} \end{cases} \quad (13)$$

Let us consider an object with rest mass m and proper radius R descending into a BH2 black hole. The constants of motion associated to t and r are [22]

$$E = -\dot{t}; \quad J = \dot{\phi}; \quad (14)$$

where

$$\begin{aligned} \dot{t} &= g_{tt} \dot{t}; \\ \dot{\phi} &= g_{\phi\phi} \dot{\phi}; \end{aligned} \quad (15)$$

In addition,

$$m^2 = -\dot{r}^2; \quad (16)$$

For simplicity we just consider the equatorial motion of the object, i.e., $\dot{\theta} = \dot{\phi} = 0$. The quadratic equation for the conserved energy E of the body coming from (14)–(16) is given by

$$E^2 - 2E + \dots = 0; \quad (17)$$

with

$$\begin{aligned} \dots &= r^2; \\ \dots &= 0; \\ \dots &= A_2(r - r_h)^2 (J^2 + m^2 r^2); \end{aligned} \quad (18)$$

The gradual approach to the black hole must stop when the proper distance from the body's center of mass to the black hole horizon equals R , the body's radius,

$$\int_{r_h}^{r_h + (R)} \frac{dr}{\sqrt{B(r)}} = R; \quad (19)$$

Integrating this equation we obtain the expression for r ,

$$\begin{cases} \frac{1}{4} C R^2 B_1 & \text{for BH1 family;} \\ R^p \frac{p}{B_3 C} & \text{for BH2 family;} \end{cases} \quad (20)$$

Solving (17) for the energy and evaluating at the point of capture $r = r_h + R$ we have

$$E_{\text{cap}} = \frac{p \frac{p}{A_2 (J^2 + m^2 r_h^2)}}{r_h} \quad (21)$$

This energy is minimal for a minimal increase in the black hole surface area, $J = 0$, such that

$$E_{\text{min}} = \frac{p}{A_2 m} \quad (22)$$

From the First Law of Black Hole Thermodynamics we know that

$$dM = \frac{1}{2} dA_r; \quad (23)$$

where A_r is the rationalized area ($A_{\text{rea}} = 4 \pi r^2$), and $dM = E_{\text{min}}$ is the change in the black hole mass due to the assimilation of the body. Thus, using (13) we obtain

$$dA_r = 2m R; \quad (24)$$

Assuming the validity of the GSL, $S_{\text{BH}}(M + dM) = S_{\text{BH}}(M) + S$, we derive an upper bound to the entropy S of an arbitrary system of proper energy E ,

$$S \leq 2\pi E R; \quad (25)$$

This result coincides with that obtained for the purely 4-dimensional Schwarzschild solution, and it is also independent of the black hole parameters [15]. It shows that the bulk does not affect the universality of the entropy bound.

Let us find now the quantum corrections to the classical BH entropy. We consider a massive scalar field in the background of a BH 2 black hole satisfying the massive Klein-Gordon equation,

$$m^2 \psi = 0; \quad (26)$$

In order to quantize this scalar field we adopt the statistical mechanical approach using the partition function Z , whose leading contribution comes from the classical solutions of the euclidean lagrangian that leads to the Bekenstein-Hawking formula. In order to compute the quantum corrections due to the scalar field we use the 't Hooft's brick wall method, which introduces an ultraviolet cutoff near the horizon, such that

$$\psi(r) = 0 \text{ at } r = r_h + \epsilon; \quad (27)$$

and an infrared cutoff very far away from the horizon,

$$\psi(r) = 0 \text{ at } r = L \gg M; \quad (28)$$

Thus, using the black hole metric (4) and the Ansatz $\psi = e^{iEt} R(r) Y_{lm}(\theta, \phi)$, Eq.(26) turns out to be

$$\frac{E^2}{A} R + \frac{r}{B} \frac{1}{A r^2} \partial_r (r^2 \frac{P}{AB} \partial_r R) - \frac{l(l+1)}{r^2} + m^2 R = 0; \quad (29)$$

Using a first order WKB approximation with $R(r) = e^{iS(r)}$ in (29) and taking the real part of this equation we can obtain the radial wave number $K = \partial_r S$ as being,

$$K = B^{-1/2} \frac{E^2}{A} - \frac{l(l+1)}{r^2} + m^2; \quad (30)$$

Now we introduce the semiclassical quantization condition,

$$n_r = \int_{r_h + \epsilon}^{r_h + L} K(r; E) dr; \quad (31)$$

In order to compute the entropy of the system we first calculate the Helmholtz free energy F of a thermal bath of scalar particles with temperature $T = 1/\beta$,

$$F = -\frac{1}{\beta} \ln Z = -\frac{1}{\beta} \ln \int_{r_h + \epsilon}^{r_h + L} dn_r \ln(1 - e^{-\beta E}); \quad (32)$$

Integrating by parts, using (30) and (31), and performing the integral in r we have

$$F = \frac{2}{3} \int_{r_h + \epsilon}^{r_h + L} dr A^{-3/2} B^{-1/2} r^2 dE \frac{(E^2 - A m^2)^{3/2}}{e^{\beta E} - 1}; \quad (33)$$

Following 't Hooft's method, the contribution of this integral near the horizon is given by

$$F \approx \frac{2r_h^3}{3} \int_{\epsilon}^L dy \frac{(A_2 r_h^2)^{3/2} (y-1)^{3/2}}{(B_3 C)^{1/2}} dE \frac{E^3}{e^{\beta E} - 1}; \quad (34)$$

where $y = r/r_h$, $\epsilon = \epsilon/r_h$, and $L = L/r_h$. Notice that since A goes to 0 near the horizon, the mass term in Eq. (33) becomes negligible.

Therefore, the leading divergent contribution to F (with $\epsilon \rightarrow 0$) is

$$F_{\text{div}} = \frac{r_h^2}{45} \frac{3}{4} \frac{(A_2)^{3/2}}{(B_3 C)^{1/2}}; \quad (35)$$

The corresponding entropy is then,

$$S_{\text{div}} = -2 \frac{\partial F}{\partial \beta} = \frac{4r_h^2}{45} \frac{3}{(B_3 C)^{1/2}}; \quad (36)$$

Using the value of the Hawking temperature $T_H = 1/\beta = 1/4\pi r_h$, with ϵ given in (13) we have

$$S_{\text{div}} = \begin{cases} r_h^2 B_1 C = (360\pi^2) & \text{for BH 1 family;} \\ r_h^2 B_3 C = (90\pi^2) & \text{for BH 2 family;} \end{cases} \quad (37)$$

We can express our result in terms of the proper thickness ϵ given by

$$S_{\text{div}} = \int_{r_h}^{r_h + \epsilon} \frac{dr}{B(r)} \begin{cases} 2\pi \frac{P}{B_1 C} & \text{for BH 1 family;} \\ \pi \frac{P}{B_3 C} & \text{for BH 2 family;} \end{cases} \quad (38)$$

Thus,

$$S_{\text{div}} = \frac{r_h^2}{90\pi^2}; \quad (39)$$

or in terms of the horizon area $A_{\text{rea}} = 4\pi r_h^2$,

$$S_{\text{div}} = \frac{A_{\text{rea}}}{360\pi^2}; \quad (40)$$

which is the same quadratically divergent correction found by 't Hooft [12] for the Schwarzschild black hole and by Nandi et al. [23] for the CFM brane black hole. Thus, we see that the correction is linearly dependent on the area.

The calculation of the entropy bound and entropy quantum correction for the BH1 black hole is similar and leads to the same results shown in (25) and (40).

IV. PERTURBATIVE DYNAMICS: MATTER AND GRAVITATIONAL PERTURBATIONS

For simplicity we model the matter field by a scalar field confined on the brane obeying the massless ($m = 0$) version of the Klein-Gordon equation (26). We expect that massive fields ($m \neq 0$) should show rather different tail behavior, but such cases will not be treated in the present paper.

Using the decomposition of the scalar field as $(t; r; \theta; \phi) = R(t; r)Y_{\ell m}(\theta; \phi)$ in terms of the angular, radial, and time variables we have the equation

$$\frac{\partial^2 R}{\partial t^2} + \frac{\partial^2 R}{\partial r^2} = V_{sc}(r(x_2))R, \quad (41)$$

with the tortoise coordinate r_* defined as

$$\frac{dr_*}{dr} = \frac{1}{A(r)B(r)}; \quad (42)$$

The effective potential V_{sc} is given by

$$V_{sc} = A(r) \frac{\ell(\ell+1)}{r^2} + \frac{1}{2r} [A(r)B^0(r) + A^0(r)B(r)]; \quad (43)$$

In order to address the problem of black hole stability under gravitational perturbations, we consider first order perturbation of $R = E$, where R and E are the Ricci tensor and the projection of the 5-dimensional Weyl tensor on the brane, respectively. In general, the gravitational perturbations depend on the tidal perturbations, namely, E . Since the complete bulk solution is not known, we shall use the simplifying assumption $E = 0$. This assumption can be justified at least in a regime where the perturbation energy does not exceed the threshold of the Kaluza-Klein massive modes. A analysis of gravitational shortcuts [24] also supports this simplification showing that gravitational fields do not travel deep into the bulk. On the other hand, since we ignore bulk back-reaction, the developed perturbative analysis should not describe the late-time behavior of gravitational perturbations. Within such premises we obtain the gravitational perturbation equation

$$R = 0; \quad (44)$$

We will consider axial perturbations in the brane geometry, following the treatment in [25]. To make this section more self contained, we will briefly describe the

treatment used in [25]. The metric Ansatz with sufficient generality is

$$ds^2 = e^2 dt^2 - e^2 dr^2 - e^2 d\Omega^2; \quad (45)$$

where we adopt here a more convenient notation,

$$e^2 = A(r); e^{2\prime} = \frac{1}{B(r)}; e^{2\prime\prime} = r^2; e^{2\prime\prime\prime} = r^2 \sin^2 \theta; \quad (46)$$

Axial perturbations in the brane metric (4) are characterized by non-null (but first order) values for δQ , δq_2 , and δq_3 in Eq. (45). We refer to [25] for further details.

In order to decouple the system, it is adopted the change of variables

$$Q = q; \quad q; \quad (47)$$

and

$$Q_0 = q_{;0}; \quad (48)$$

with $;$ = 2;3. We denote partial differentiation with respect to t , and by $\prime, \prime\prime, \prime\prime\prime$, respectively. The perturbations are then described by

$$(e^{3\prime} + e^{2\prime} Q_{23})_{;3} e^{3\prime} + e^{3\prime\prime} = (\delta Q_{;2})_{;0}; \quad (49)$$

$$(e^{3\prime} + e^{2\prime} Q_{23})_{;2} e^{3\prime} + e^{3\prime\prime} = (\delta Q_{;3})_{;0}; \quad (50)$$

Setting $Q(t; r) = \exp(\beta + \gamma) Q_{23}$, Eqs.(49) and (50) can be combined as

$$r^4 \frac{B(r)}{A(r)} \frac{\partial}{\partial r} \frac{1}{r^2} \frac{\partial Q}{A(r)B(r)} \frac{\partial Q}{\partial r} = r^2 \frac{B(r)}{A(r)} \frac{\partial^2 Q}{\partial t^2} = \sin^3 \theta \frac{\partial}{\partial \theta} \frac{1}{\sin^3 \theta} \frac{\partial Q}{\partial \theta}; \quad (51)$$

We further separate variables and write Eq.(51) in the form of a Schrodinger-type wave equation by introducing $Q(t; r) = rZ(t; r)C_{\ell+2}^{3=2}(\theta)$, and $r = r(x_2)$, where $C_{\ell+2}^{3=2}(\theta)$ is the Gegenbauer function. Thus, the axial gravitational perturbations are given by an equation of motion with the form given in (41) with the effective potential

$$V_{grav}(r) = A(r) \frac{\ell(\ell+2)(\ell-1)}{r^2} + \frac{2A(r)B(r)}{r^2} \frac{1}{2r} [A(r)B^0(r) + A^0(r)B(r)]; \quad (52)$$

V. SPECIFIC MODELS

A. Overview of the results

The equations of motion for the scalar and axial gravitational perturbations give us a tool to analyze the dynamics and stability of the black hole solutions in both the CFM and "zero mass" black hole backgrounds. Of particular interest are the quasinormal modes. They are defined as the solutions of Eq. (41) which satisfy both boundary conditions that require purely out-going waves at (brane) spatial infinity and purely in-going waves at the event horizon,

$$\lim_{x \rightarrow 1} x^{\frac{1}{2}} e^{-i\omega x} = \text{constant}; \quad (53)$$

with $\psi = R \cdot$ and $Z \cdot$ for the scalar and gravitational perturbations, respectively.

In order to analyze quasinormal mode phase and late-time behavior of the perturbations, we apply a numerical characteristic integration scheme based in the light-cone variables $u = t - r_*$ and $v = t + r_*$ used, for example, in [26, 27, 28]. In addition, to check some results obtained in "time-dependent" approach we employ the semi-analytical WKB-type method developed in [29] and improved in [30]. Both approaches show good agreement for the fundamental overtone which is the dominating contribution in the signal for intermediate late-time.

At a qualitative level we have observed the usual picture in the perturbative dynamics for all fields and geometries considered here. After the initial transient regime, it follows the quasinormal mode phase and finally a power-law tail. In contrast to the 5-dimensional model in [31], in the present context we do not observe Kaluza-Klein massive modes in the late-time behavior of the perturbations. This is actually expected, since our treatment for gravitational perturbations neglects the back-reaction from the bulk. Still, as discussed in section IV, our results should model the quasinormal regime.

A necessary condition for the stability of the geometries we have considered is that these backgrounds must be stable under the perturbations modelled by the effective potentials (43) and (52).

If the effective potential (V) is positive definite, the differential operator

$$D = \frac{\partial^2}{\partial r_*^2} + V \quad (54)$$

is a positive self-adjoint operator in the Hilbert space of square integrable functions of r_* , and, therefore, all solutions of the perturbative equations of motion with compact support initial conditions are bounded.

However, as we will see, the effective potentials may be non-positive definite for certain choices of the parameters in Eqs.(9)–(10). Nevertheless, even when the effective potential is not positive definite, we do not observe unbounded solutions.

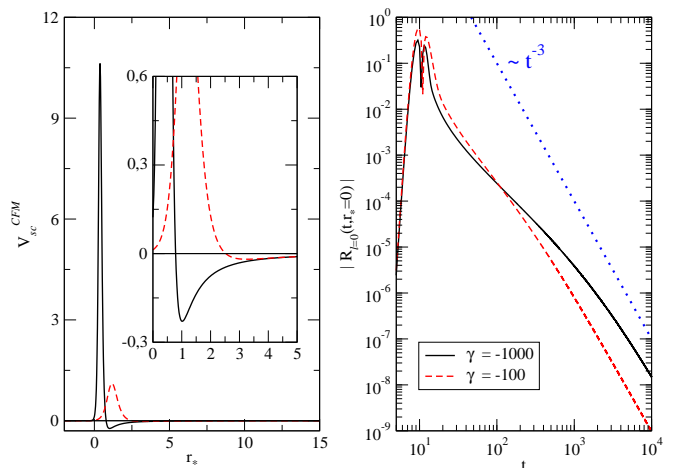


Figure 1: (Left) Effective potential for the scalar perturbations in the CFM background for very negative values of γ . Negative peaks are displayed in detail. (Right) Bounded evolution of the scalar field perturbation with such effective potentials. The dotted line is the late-time power-law tail. The parameters are $\ell = 0$ and $M = 1$.

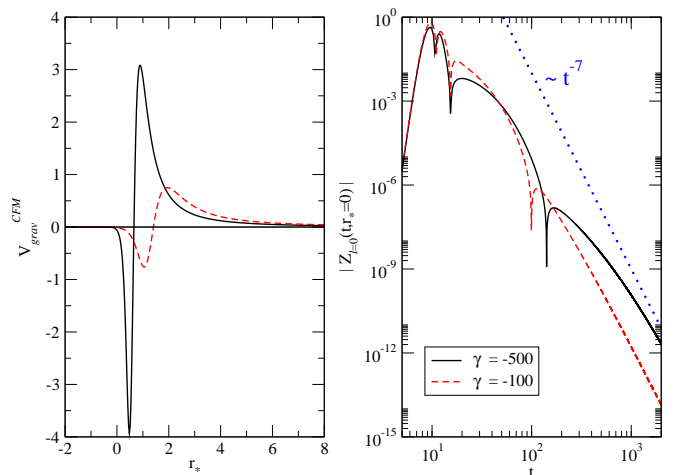


Figure 2: (Left) Effective potential for the axial gravitational perturbations in the CFM background for very negative values of γ . (Right) Bounded evolution of the gravitational field perturbation with such effective potentials. The dotted line is the late-time power-law tail. The parameters in the graphs are $\ell = 2$ and $M = 1$.

Using both high order WKB method and direct numerical integration of the equations of motion a numerical search for quasinormal modes with positive imaginary part was performed for scalar and gravitational perturbations. One of the most important results in this work is that no unstable mode was observed. Furthermore, the perturbative late-time tails have power-law behavior (in one case an oscillatory decay with power-law envelope).

Table I: Fundamental quasinormal frequencies for the scalar perturbation around the CFM black hole for several values of the parameters ν and ℓ . The black hole mass is set to $M = 1$.

ℓ	ν	Direct Integration		WKB-3 th order		WKB-6 th order	
		Re(ω_0)	-Im(ω_0)	Re(ω_0)	-Im(ω_0)	Re(ω_0)	-Im(ω_0)
1	-5	0.28580	0.19779	0.208204	0.225080	0.305499	0.181027
1	-2	0.29201	0.16608	0.276143	0.181776	0.309350	0.122589
1	0	0.29337	0.14138	0.299359	0.154590	0.236213	0.165871
1	1	0.29400	0.12853	0.298384	0.134468	0.252449	0.171879
1	2	0.29415	0.11378	0.294679	0.115208	0.293168	0.120632
1	3	0.29283	0.098045	0.291114	0.0980014	0.292910	0.0977616
1	3.9	0.29076	0.082598	0.287181	0.0820285	0.289628	0.0811812
2	-5	0.48053	0.18951	0.488726	0.207518	0.433498	0.183580
2	-2	0.48266	0.16069	0.488518	0.166137	0.451478	0.193079
2	0	0.48413	0.13815	0.486195	0.139258	0.485925	0.142572
2	1	0.48449	0.12570	0.485289	0.126043	0.485911	0.126758
2	2	0.48447	0.11206	0.484420	0.112159	0.484691	0.112283
2	3	0.48317	0.097097	0.483211	0.09680485	0.483642	0.0967661
2	3.9	0.48178	0.080778	0.481091	0.08098300	0.481705	0.0808983

Table II: Fundamental quasinormal frequencies for the axial gravitational perturbation around the CFM black hole for several values of the parameters ν and ℓ . The black hole mass is set to $M = 1$.

ℓ	ν	Direct Integration		WKB-3 th order		WKB-6 th order	
		Re(ω_0)	-Im(ω_0)	Re(ω_0)	-Im(ω_0)	Re(ω_0)	-Im(ω_0)
2	-5	0.36409	0.18017	0.401345	0.197274	0.418575	0.193276
2	-2	0.37049	0.16062	0.391442	0.163223	0.402747	0.163222
2	0	0.37359	0.13539	0.384611	0.137147	0.389781	0.139044
2	1	0.37457	0.12138	0.381053	0.122624	0.383017	0.124656
2	2	0.37483	0.10604	0.377306	0.106767	0.377126	0.107996
2	3	0.37368	0.088957	0.373162	0.0892174	0.373619	0.0888910
2	3.9	0.36961	0.072435	0.368552	0.0717786	0.371935	0.0712303
3	-5	0.59476	0.18365	0.608026	0.191340	0.613069	0.194241
3	-2	0.59835	0.15845	0.604567	0.159482	0.605032	0.161682
3	0	0.59993	0.13527	0.602594	0.135600	0.601901	0.136695
3	1	0.60033	0.12238	0.601646	0.122520	0.601033	0.123070
3	2	0.60026	0.10832	0.600614	0.108374	0.600375	0.108525
3	3	0.59947	0.092690	0.599265	0.0927284	0.599443	0.0927025
3	3.9	0.59700	0.077176	0.597227	0.0767434	0.597584	0.0767411

B. CFM brane black holes

We first consider scalar perturbations in the CFM scenario. The tortoise coordinate r_* after the explicit integration is

$$r_* = T_1(r) + T_2(r) + T_3(r) \quad (55)$$

with

$$T_1(r) = \frac{1}{2} \frac{r^{2p}}{(2r - M)(2r - 3M)}; \quad (56)$$

$$T_2(r) = \frac{M(5 + \nu)}{4} \ln [4r - M(3 + \nu) + 2T_1(r)]; \quad (57)$$

$$T_3(r) = \frac{2M}{4} \ln \frac{M(5 + \nu)r - M^2(6 + \nu) + M^{2p} \frac{r^{2p}}{4}}{r - 2M} T_1(r); \quad (58)$$

The scalar and axial gravitational effective potentials for perturbations in the CFM background (respectively, V_{sc}^{CFM} and V_{grav}^{CFM}) in terms of the parameters M and ℓ are given by

$$V_{sc}^{CFM}(r) = 1 - \frac{2M}{r} - \frac{\ell(\ell+1)}{r^2} + \frac{2M}{r^3} + \frac{M(3\ell^2 - 6M\ell + 6M^2)}{r^3(2r - 3M)} \quad (59)$$

and

$$V_{grav}^{CFM}(r) = 1 - \frac{2M}{r} - \frac{\ell(\ell+1)}{r^2} - \frac{6M}{r^3} - \frac{M(3\ell^2 - 20M\ell + 18M^2)}{r^3(2r - 3M)} \quad (60)$$

Setting $\ell = 3$ we recover the usual expressions for perturbations around the four dimensional Schwarzschild black hole.

A basic feature of the effective potentials V_{sc}^{CFM} and V_{grav}^{CFM} is that they are not positive definite. Typically, for negative enough values of the parameter ℓ (with large j) a negative peak in the effective potential will show up. It is no longer obvious that the scalar and gravitational perturbations will be stable.

If the effective potential is not positive definite (and cannot be approximated by a positive definite one), the WKB semi-analytical formulae will usually not be applicable, but direct integration techniques will. Using the later approach an extensive search for unstable solutions was made. One important result in this work is that even for very high values of ℓ , the (scalar and gravitational) perturbative dynamics is always stable. This is illustrated in Figs. 1 and 2, where we show non-positive definite effective potentials and the corresponding (bounded) field evolution.

The overall picture of the perturbative dynamics for the effective potentials hereby considered is the usual one. After a brief transient regime, the quasinormal mode dominated phase follows, and, finally, at late times a power-law tail dominates.

For the fundamental multipole mode ($\ell = 0$) the effective potential will not be positive definite for any value of the parameter ℓ . Direct integration shows that the field evolution is always bounded for a great range of variation of ℓ . This point is illustrated in Figs. 1 and 2, where we have selected rather large values of ℓ . Indeed, it is observed that the decay is dominated from very early time by the power-law tail. Therefore, it is very difficult to estimate the quasinormal frequencies directly from this "time-dependent" approach. The WKB-type expressions are not applicable if $\ell = 0$ for two reasons: the effective potentials are not positive for r larger than a certain value, and it is well known that this method works better with $\ell < n$, where n is the overtone number.

With small but non-zero values of ℓ the quasinormal frequencies can be accurately estimated. As it is shown in

Tables I and II, the concordance with the WKB results is reasonable, except for some values of ℓ (typically around $\ell = 0$).

For large values of ℓ an analytical expression for the quasinormal frequencies can be obtained. Expanding the effective potential in terms of small values of $1/\ell$ and using the WKB method in the lowest order (which is exact in this limit) we find

$$\text{Re}(\omega_n) = \frac{\ell}{3} - \frac{1}{3M} \quad (61)$$

$$\text{Im}(\omega_n) = -\frac{2\ell}{3M^2} \left(n + \frac{1}{2} \right) \quad (62)$$

As it can be seen from the data in tables I and II and Fig. 3, the dependence of the frequencies with the parameter ℓ is very weak, although not trivial. In a large variation range of the absolute value of $\text{Im}(\omega_0)$ is a monotonically decreasing function, while $\text{Re}(\omega_0)$ typically has maximum points.

The late-time behavior of the perturbations considered here can be treated analytically. Far from the black hole the scalar effective potential in terms of r_* assumes the form,

$$V_{sc}^{CFM}(r_*) = \begin{cases} \frac{2M}{r_*^3} & \text{with } \ell = 0 \\ \frac{\ell(\ell+1)}{r_*^2} + \frac{4M\ell(\ell+1)\ln(r_* - 2M)}{r_*^3} & \text{with } \ell > 0 \end{cases} \quad (63)$$

It is then shown [32, 33] that with the initial data having compact support a potential with this form has a late-time tail

$$R_{\ell}^{CFM} \sim t^{-(2\ell+3)} \quad (64)$$

Therefore, at asymptotically late times the perturbation decays as a power-law tail for any value of the parameter ℓ . This is a strong indication that the models are indeed stable. This point is illustrated in Figs. 1 and 2. It is reminiscent from a similar behavior of the Gauss Bonnet term added to Einstein gravity in higher dimensions, which was recently treated in [34]. Although the result is formally valid also for the gravitational perturbations we have considered, it should be noted that in the simplified model developed in this paper the back-reaction from the bulk, which can modify the tail presented here, was neglected.

C. "Zero mass" brane black holes

The treatment in section IV is general enough to include also the case of perturbations around the "zero mass" brane black hole. Using the metric (10) the scalar and axial gravitational perturbations are described by wave equations similar to Eq.(41) with

Table III: Fundamental quasinormal frequencies for the scalar perturbation around the "zero mass" black hole for several values of the C and ν . The parameter h is set to $h = 1$.

ν	C	Direct Integration		WKB-3 th order		WKB-6 th order	
		$\text{Re}(\omega_n)$	$-\text{Im}(\omega_n)$	$\text{Re}(\omega_n)$	$-\text{Im}(\omega_n)$	$\text{Re}(\omega_n)$	$-\text{Im}(\omega_n)$
1	0	–	–	0.728358	0.232800	0.746504	0.230697
1	0.1	0.74494	0.24551	0.730716	0.247607	0.749727	0.245155
1	0.5	0.75196	0.30135	0.732795	0.303801	0.755273	0.301191
1	0.9	0.75437	0.35023	0.726005	0.356124	0.751242	0.357060
1	1.0	0.75410	0.36201	0.722899	0.368853	0.748461	0.371463
1	1.1	0.75354	0.37352	0.719182	0.381471	0.745143	0.385894
1	2.0	0.74548	0.46711	0.660519	0.494129	0.732352	0.479133
2	0	–	–	1.242071	0.230667	1.246220	0.231061
2	0.1	1.24534	0.21001	1.243863	0.245695	1.248248	0.246014
2	0.5	1.25534	0.28301	1.246290	0.299897	1.251377	0.300033
2	0.9	1.25072	0.34681	1.244715	0.347044	1.250452	0.347062
2	1.0	1.24989	0.35677	1.243914	0.358055	1.249839	0.358066
2	1.1	1.25377	0.36031	1.242968	0.368816	1.249090	0.368835
2	2.0	1.24523	0.44843	1.227403	0.456844	1.235779	0.459396

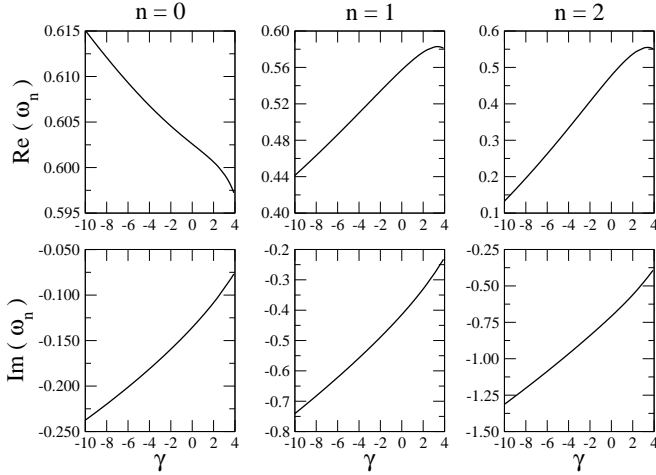


Figure 3: Dependence of gravitational perturbation quasinormal frequencies on γ in the CFM geometry. The results are qualitatively similar for the scalar perturbation. The parameters are $\nu = 3$ and $M = 1$.

effective potentials given by

$$V_{sc}^{zm}(r) = 1 - \frac{h^2}{r^2} - \frac{\nu(\nu+1)}{r^2} + \frac{2h^2}{r^4} + \frac{C}{(2r^2 - h^2)^{3=2}} - 1 - \frac{5h^2}{r^2} + \frac{2h^4}{r^4} ; \quad (65)$$

and

$$V_{grav}^{zm}(r) = 1 - \frac{h^2}{r^2} - \frac{\nu(\nu+1)}{r^2} - \frac{4h^2}{r^4} + \frac{C}{(2r^2 - h^2)^{3=2}} - 5 - \frac{11h^2}{r^2} + \frac{4h^4}{r^4} ; \quad (66)$$

Again, the effective potentials can be non-positive definite for specific choices of parameters, as illustrated in Fig. 4 (left). For example, if $\nu = 0$ and $C > h$, V_{sc}^{zm} will not be positive definite. If $\nu > 0$, V_{sc}^{zm} and V_{grav}^{zm} will be non-positive definite for high enough values of C .

Except for $C = h$, an explicit expression for the tortoise coordinate was not found. Nevertheless, the numerical integration is possible. The semi-analytical WKB approach was also used to compute quasinormal frequencies. The concordance is excellent. The WKB formulas seem to be more reliable in the present case. With the choice $C = 1$ we recover some results considered in [21]. Again, an extensive search for unstable modes was performed. Some calculated frequencies are shown in Tables III and IV. Our results show that the dynamics of the scalar and axial gravitational perturbations is always stable in the "zero mass" background. We illustrate this point in Figs. 4 and 5.

Analytical expressions for the quasinormal frequencies for the scalar and gravitational perturbations can be obtained in the limit of large multipole index ν . As done in the CFM geometry, we obtain

$$\text{Re}(\omega_n) = \frac{\nu}{2h} ; \quad (67)$$

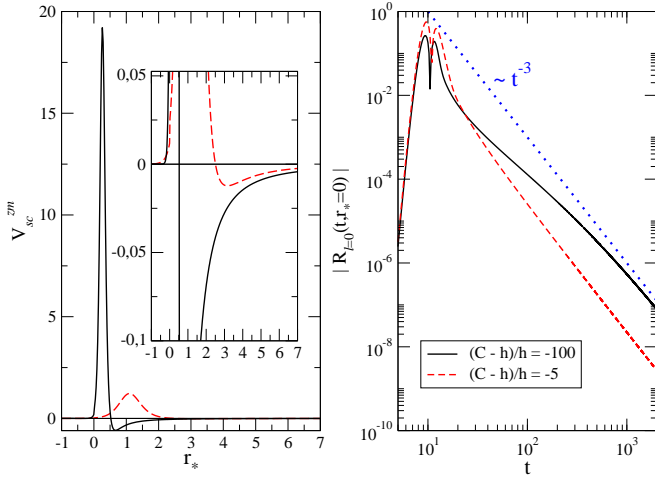


Figure 4: (Left) Effective potential for the scalar perturbations in the “zero mass” black hole background with high values of C . Negative peaks are displayed in detail. (Right) Bounded evolution of the scalar field perturbation with such effective potentials. The dotted line is the late-time power-law tail. The parameters are $\ell = 0$ and $h = 1$.

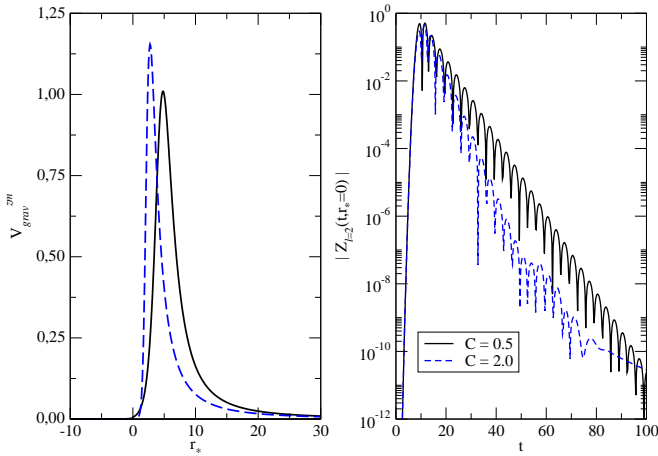


Figure 5: (Left) Typical effective potential for the gravitational perturbations in the “zero mass” black hole background. (Right) Bounded evolution of the gravitational field perturbation with such effective potentials. The parameters are $\ell = 2$ and $h = 1$.

$$\text{Im}(\omega_n) = -\frac{\nu}{2h} \left(n + \frac{1}{2} \right) : \quad (68)$$

We expect that the late-time behavior of the gravitational perturbations should be dominated by back scattering from the bulk, not considered here. But the tail contribution to the scalar decay can be analytically treated, at least in the limit where $r \gg h$. In this case if $C > h$ or $0 < C < h$, the effective potential V_{sc}^{zm} is

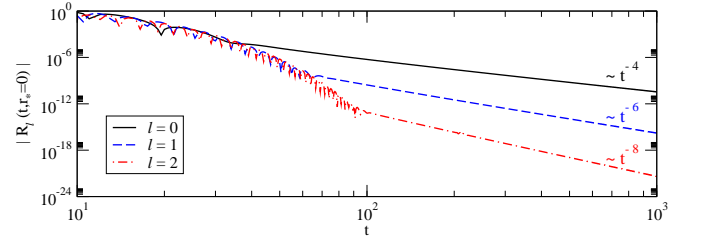


Figure 6: Bounded evolution of the scalar field perturbation in the “zero mass” black hole background with $C = h$ for several values of ℓ . After the quasinormal mode phase a power-law tail is observed. The tail dependence with ℓ obeys Eq. (73). In the graphs the parameter h was set to $h = 1$.

approximated by

$$V_{sc}^{zm}(r_*) \approx \begin{cases} \frac{C-h}{2r_*^3} & \text{with } \ell = 0; \\ \frac{\ell(\ell+1)}{r_*^2} + \frac{2(C-h)\ell(\ell+1)\ln(r_*=h)}{2r_*^3} & \text{with } \ell > 0; \end{cases} \quad (69)$$

Again, we observe that (32, 33) with the initial data having compact support the tail has the form

$$R_{\ell}^{zm} \sim t^{-(2\ell+3)} \text{ with } 0 < C < h \text{ or } C > h : \quad (70)$$

An interesting limit is when $C = h$. In this case the explicit expression for the tortoise coordinate according to the usual definition in Eq. (42) is

$$r_*(r) = r + \frac{h}{2} \ln \left| \frac{r}{h} - 1 \right| - \frac{h}{2} \ln \left| \frac{r}{h} + 1 \right| : \quad (71)$$

The effective potential V_{sc}^{zm} with $C = h$ is approximated by

$$V_{sc}^{zm}(r_*) \approx \begin{cases} \frac{2h^2}{r_*^4} & \text{with } \ell = 0; \\ \frac{\ell(\ell+1)}{r_*^2} - \frac{2\ell(\ell+1)h^2}{r_*^4} & \text{with } \ell > 0; \end{cases} \quad (72)$$

In this limit a power-law still dominates the late-time decay. But its dependence with the multipole index ℓ is different,

$$R_{\ell}^{zm} \sim t^{-(2\ell+4)} \text{ with } C = h : \quad (73)$$

This point is illustrated in Fig. 6.

As observed in the CFM model, for the non-extreme “zero mass” model the scalar perturbation decays as a power-law tail suggesting that the model is stable.

The qualitative picture of the field evolution in the “zero mass” black hole quasinormal mode followed by power-law tail changes drastically when the extreme case ($C = 0$) is considered (see Fig. 7). If $\ell = 0$, we observe the usual power-law tail dominating the late-time decay. But when $\ell > 0$, the simple power-law tail is replaced by an oscillatory decay with a power-law envelope,

$$R_{\ell}^{zm} \sim t^{-3-2\ell} \sin(\omega_{\ell} t) \text{ with } C = 0 \text{ and } \ell > 0 : \quad (74)$$

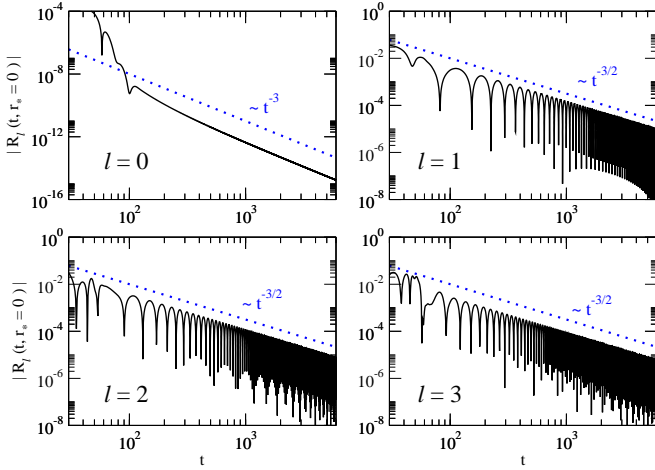


Figure 7: Bounded evolution of the scalar field perturbation in the extreme “zero mass” black hole background ($C = 0$), for several values of ν . If $\nu = 0$, the decay is dominated by a power-law tail (t^{-3}). If $\nu > 0$, the decay is dominated by an oscillatory tail, whose envelope is $t^{-3/2}$. In the graphs the parameter h was set to $h = 1$.

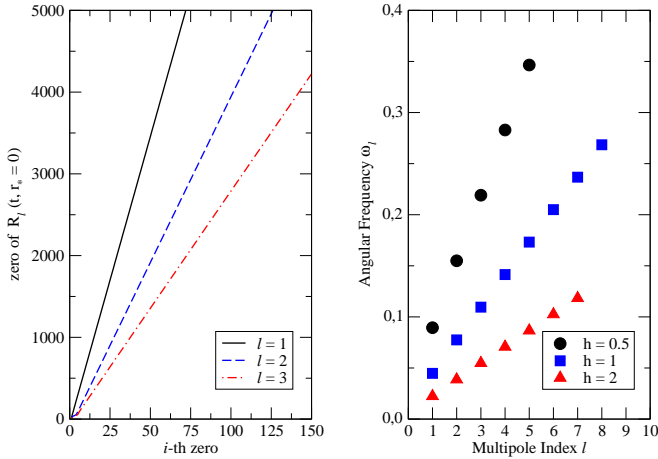


Figure 8: (Left) Numerical value of t where the scalar wave function is zero in the extreme “zero mass” black hole. Straight lines imply that the period of oscillation is a constant. The parameter h is set to $h = 1$. (Right) Dependence of the angular frequency ω_l in Eq.(74) with ν for several values of h .

Therefore, for $\nu > 0$ the power index ($-3/2$) is independent of the multipole index ν . The angular frequency ω_l for large times approaches a constant, as we can see in Fig. 8 (left). The angular frequency is well approximated by a linear function of ν , as indicated in Table V for some values of h . This result implies that the dominating contributions in the late-time decay are the modes with $\nu > 0$, i.e., the power-law enveloped oscillatory terms. We also observe that these tails dominate from very early times, so that it was not possible to estimate the quasinormal frequencies in the extreme case (as indicated in the first lines of Tables III and IV).

VI. CONCLUSIONS

In this work we studied brane black holes from the point of view of a brane observer. We considered the two family solutions found by Bronnikov et al. [9] in order to derive the Bekenstein entropy bound and the one-loop correction to the Bekenstein-Hawking formula using the ‘t Hooft brickwall method. In addition, we performed scalar and axial gravitational perturbations in two specific examples of these families. With these perturbations we were able to analyze the dynamics and stability of the black hole solutions.

The results of the black hole thermodynamics study show that the entropy bound continues to be independent of the black hole parameters. Thus, the presence of the bulk does not affect the universality of the entropy bound for a brane observer, as ourselves, reinforcing the Generalized Second Law. Moreover, applying the ‘t Hooft’s brickwall method to both black hole families we see that the entropy correction takes the same form as that of a Schwarzschild black hole when written in terms of its own black hole parameters. Therefore, as the correction is linearly dependent on the area, it can be absorbed in a renormalized gravitational constant.

One of the most important results in this paper came from the perturbative dynamics. We should stress that the assumption $E = 0$ was necessary in order to solve the gravitational perturbation equation (44) without any knowledge of the bulk structure. This vanishing tidal effect is perfectly justified when the perturbation energy is lower than the threshold of the Kaluza-Klein massive modes. Likewise, as we neglect the bulk back-reaction, our analysis does not describe the perturbation late-time behavior. Our results show no unstable mode in the scalar and gravitational analysis. In addition, the late-time tails display a power-law behavior what enforces their stability.

In the case of CFM black hole even if the effective potential is not positive (define the quasinormal modes are stable (negative imaginary part). The agreement of the several methods employed in the calculation is good for ν not too small.

On the other hand, in the case of the “zero mass” black hole we observe a richer picture. The scalar and gravitational field evolution is always bounded suggesting that this class of models is stable. But the late-time decay of the matter field strongly depends on the parameters C and h . If C is non-zero and not equal to h , the late-time decay is dominated by a power-law tail with the usual dependence on the multipole parameter ν . But if $C = h$, this dependence changes. Finally, in the extreme regime ($C = 0$) the late-time decay is dominated by oscillatory modes with a power-law envelope. This power index seems to be universal, not depending on ν .

Summarizing, the thermodynamics in the class of models we considered is consistent, while the dynamics in specific backgrounds is stable in the approach employed in the present work.

Table IV : Fundamental quasinormal frequencies for the axial gravitational perturbation around the "zero mass" black hole for several values of the C and ν . The parameter h is set to $h = 1$.

ν	C	Direct Integration		WKB-3 th order		WKB-6 th order	
		$\text{Re}(\omega_0)$	$-\text{Im}(\omega_0)$	$\text{Re}(\omega_0)$	$-\text{Im}(\omega_0)$	$\text{Re}(\omega_0)$	$-\text{Im}(\omega_0)$
2	0	–	–	0.934530	0.191198	0.934386	0.219631
2	0.1	0.94412	0.21924	0.935381	0.205749	0.964066	0.215448
2	0.5	0.94783	0.26533	0.938066	0.264005	0.958654	0.249590
2	0.9	0.94334	0.30949	0.942035	0.318153	0.929971	0.317851
2	1.0	0.94207	0.31993	0.943255	0.330875	0.928449	0.334460
2	1.1	0.94069	0.33016	0.944551	0.343278	0.928937	0.350243
2	2.0	0.92442	0.41343	0.958486	0.442675	0.973998	0.456121
3	0	–	–	1.537001	0.214671	1.538619	0.215204
3	0.1	1.50122	0.25435	1.537512	0.229197	1.539283	0.229786
3	0.5	1.53958	0.27762	1.536138	0.280829	1.538697	0.280900
3	0.9	1.53905	0.32341	1.532735	0.325500	1.534597	0.324529
3	1.0	1.53757	0.33402	1.531809	0.335949	1.533070	0.334820
3	1.1	1.53594	0.34411	1.530883	0.346171	1.531369	0.344973
3	2.0	1.52161	0.42100	1.523732	0.430806	1.513596	0.433952

Table V : Oscillatory frequency of the tail in the extreme "zero mass" ($C = 0$) black hole for several values of h .

h	Angular Frequency ω_0 ($\nu > 0$)
0.5	$0.02593 + 0.06421 i$
1.0	$0.01347 + 0.03191 i$
2.0	$0.006683 + 0.01597 i$

While our results suggest that the brane models presented are viable, the final check would be the

analysis of the continuation in the bulk of the geometries presented here.

Acknowledgments

This work was partially supported by Fundacao de Amparo a Pesquisa do Estado de São Paulo (FAPESP) and Conselho Nacional de Desenvolvimento Científico e Tecnológico (CNPq).

-
- [1] T. Kaluza, *Sitzungsberichte Preussische Akademie der Wissenschaften* K 1, 966 (1921); O. Klein, *Z. F. Physik* 37, 895 (1926); O. Klein, *Nature* 118, 516 (1926).
- [2] J. Polchinski, *Superstring Theory Vols. 1 and 2*, Cambridge University Press (Cambridge, 1998).
- [3] L. Randall and R. Sundrum, *Phys. Rev. Lett.* 83, 3370 (1999); *Phys. Rev. Lett.* 83, 4690 (1999).
- [4] A. Chamblin, S.W. Hawking, H.S. Reall, *Phys. Rev. D* 61, 065007 (2000).
- [5] R. Gregory and R. Laamame, *Phys. Rev. Lett.* 70, 2837 (1993).
- [6] R. Casadio, A. Fabbri, and L. Mazzacurati, *Phys. Rev. D* 65, 084040 (2002).
- [7] R. Casadio and L. Mazzacurati, *Mod. Phys. Lett. A* 18, 651 (2003).
- [8] T. Shiromizu, K. Maeda and M. Sasaki, *Phys. Rev. D* 62, 024012 (2000).
- [9] K.A. Bronnikov, H. Dehren, and V.N. Melnikov, *Phys. Rev. D* 68, 024025 (2003).
- [10] J.D. Bekenstein, *Phys. Rev. D* 7, 949 (1973).
- [11] S.W. Hawking, *Commun. Math. Phys.* 43, 199 (1975).
- [12] G. 't Hooft, *Nucl. Phys. B* 256, 727 (1985).
- [13] E. Abdalla and L.A. Correa Borbonet, *Mod. Phys. Lett. A* 16, 2495 (2001).
- [14] L. Susskind and J. Uglum, *Phys. Rev. D* 50, 2700 (1994).
- [15] J.D. Bekenstein, *Phys. Rev. D* 23, 287 (1981).
- [16] K.A. Bronnikov and Sung-Won Kim, *Phys. Rev. D* 67, 064027 (2003).
- [17] Ruth Gregory, Richard Whisker, Kris Beckwith, Chris Done *Journal of Cosmology and Astroparticle Physics* 13, 0410 (2004).
- [18] C. Gemani and R. Maaertens, *Phys. Rev. D* 64, 124010 (2001).
- [19] N. Dadhich, R. Maaertens, Ph. Papadopoulos, V. Rezanina, *Phys. Lett. B* 487, 1 (2000); A.N. Aliiev, A.E. Gumrukcuoglu, *Class. Quant. Grav.* 21, 5081 (2004); A.N. Aliiev, A.E. Gumrukcuoglu, *Phys. Rev. D* 71, 104027 (2005).

- [20] G. Konas, E. Papantonopoulos, I. Pappa, Phys. Rev. D 66, 104014 (2002). G. Konas, E. Papantonopoulos, V. Zamarias, Phys. Rev. D 66, 104028 (2002).
- [21] P. Kanti and R. Konoplya, Phys. Rev. D 73, 044002 (2006).
- [22] B. Carter, Phys. Rev. 174, 1559 (1968); R. Hojn an and S. Hojn an, Phys. Rev. D 15, 2724 (1977); B. Linet, Gen. Rel. Grav. 31, 1609 (1999); S. Hod, Phys. Rev. D 61, 024023 (2000); *ibid.* Phys. Rev. D 61, 024018 (2000); J. D. Bekenstein and A. E. Mayo, Phys. Rev. D 61, 024022 (2000); Bin Wang, Elcio Abdalla, Phys. Rev. D 62, 044030 (2000); Weigang Qiu, Bin Wang, Ru-Keng Su, Elcio Abdalla, Phys. Rev. D 64, 027503 (2001).
- [23] K. Nandi, Y.-Z. Zhang, A. Bhadra and P. Mitra, Int. J. Mod. Phys. A 21, 2519 (2006).
- [24] Elcio Abdalla, Bertha Cuadros-Melgar, Sze-Shiang Feng, Bin Wang, Phys. Rev. D 65, 083512 (2002); Elcio Abdalla, A denauer G. Casali, Bertha Cuadros-Melgar, Int. J. Theor. Phys. 43, 801 (2004).
- [25] S. Chandrasekhar, The Mathematical Theory of Black Holes, Oxford University Press (New York, 1983).
- [26] C. Gundlach, R. Price, and J. Pullin, Phys. Rev. D 49, 883 (1994).
- [27] C. Molina, Phys. Rev. D 68, 064007 (2003).
- [28] Bin Wang, C. Molina, Elcio Abdalla, Phys. Rev. D 63, 084001 (2001); C. Molina, D. Giugno, E. Abdalla, A. Saa, Phys. Rev. D 69, 104013 (2004).
- [29] B. F. Schutz and C. M. Will, Astrophys. J. 291, L33 (1985).
- [30] S. Iyer and C. M. Will, Phys. Rev. D 35, 3621 (1987); R. A. Konoplya, Phys. Rev. D 68, 024018 (2003).
- [31] Sanjeev S. Seahra, Chris Clarkson, Roy Maartens, Phys. Rev. Lett. 94, 121302 (2005).
- [32] R. H. Price, Phys. Rev. D 5, 2419 (1974).
- [33] E. S. C. Ching, P. T. Leung, W. M. Suen and K. Young, Phys. Rev. D 52, 2118 (1995).
- [34] E. Abdalla, R. Konoplya, and C. Molina, Phys. Rev. D 72, 084006 (2005).